00

Infra-red spectroscopy of reflection-absorbance with account for thin surface layers: the theoty and experiment

© A.V. Michailov[1], A.V. Povolotskiy[1], V.L. Kuzmin[2]

[1] St. Petersburg State University,
198504 St. Petersburg, Russia
[2] Peter the Great Saint-Petersburg Polytechnic University,
195251 St. Petersburg, Russia

e-mail: mav030655@gmail.com, apov@inbox.ru, kuzmin_vl@mail.ru

Received 2023
Revised 2023
Accepted 2024

The description of the reflectance-absorbance spectra for the light reflecting from the plane boundary between absorbing liquid phase and the gaseous one is developed accounting a thin anisotropic absorbing interfacial layer. The surface contributions are shown being described in terms of four integral parameters of the permittivity profiles universal respectively of the incidence angle and the type of profile. The results of performed studies of angular dependency of the reflectance-absorbance spectra in the infra red region for the lipid on the water- gas interface are in a fair agreement numerically with the model considered.

Keywords: Plane interface boundary, reflectance-absorbance, permittivity.

DOI: 10.61011/EOS.2024.02.58453.5620-23

Introduction

Use of the optical methods to study the absorbing surface layers and films, among which one of the most common is the reflection absorption spectroscopy (IRRAS — infrared reflection absorption spectroscopy), continues to be of intense interest both from the fundamental or applied points of view. The thin layers and films are studied, provided that the layer thickness is small: $L \ll \lambda$, where λ — wavelength of the incident radiation, L — specific thickness of the layer. Despite the smallness of the parameter L/λ, the specified methods make it possible to effectively determine the surface corrections to the reflection coefficients both in the infrared and in the visible areas of the spectrum. The study results are relevant in different applications both on the surface of liquid media, for example, surface layers and films of surfactants [1–3], polymers [4,5], DNA [6–8], proteins and lipids [9–12], and on the surface of hard media, for example, metals [13–15].

During interpretation of the experimental data of reflection absorption spectroscopy the authors quite often restrict themselves to discussion of appearance or absence of the bands, and also their variation in certain experimental situations. In quantitative description, usually an approach is used, when initially a surface layer (SL) model is created, and its parameters are varied to achieve the compliance between the experimental and calculated spectra of optical density. Besides, the question of how many independent parameters this model may contain remains out of consideration. Such approach is also used for interpretation of multi-angle data [9,16–22]. Intuitively it seems evident that the analysis of multi-angle dependences increases the reliability of the calculation results and may enable production of the additional information. However, the question of the range of angles and the number of spectra necessary and sufficient for the valid interpretation of data remains out of discussion.

The simplest SL model is a homogeneous film with thickness of L between two half-infinite media. There is a well known analytical solution [23] for this model, making it possible to relate the material and the imaginary parts of the SL refraction index and its thickness with the reflection coefficients of polarized radiation. This approximation is widely used for numerical calculations, however, the bulkiness of the final expressions for the reflection coefficients complicates the clear analytical discussion of the produced results [24]. The papers [24–29] simplified this approach in the assumption $L/\lambda \ll 1$.

In the theoretical description of the radiation reflection with account of interphase layers the effective approach was the molecular-statistical one [16,30–33], which was used in the large number of papers [9,18,34–38]. It is material that it is not necessary to preset the profiles of local values characteristics, such as the material and imaginary components of the dielectric permittivity when using this approach. Before it was shown that the use of this approach for s-polarization [39] makes it possible to produce the expressions for the reflective capacity and optical density, which contain only one parameter determined by the profile of dielectric permittivity in SL. This fact makes it possible, using the measurement of these values at one angle of incidence, to predict them at any other angle. Therefore, it was shown that this parameter is an angular invariant. It should be emphasized that in this paper we consider the

case of external reflection of electromagnet wave, the case of the internal reflection was considered, for example, in [40].

This paper considers the reflection of *p*-polarized light, it is demonstrated that the reflective capacity and optical density in this case are determined by three parameters determined by the profile of dielectric permittivity, accordingly, for the determination of angular dependences of these values it is necessary to measure the reflection-absorption spectra at three angles of incidence. The possibility to determine only three parameters on the basis of the experiment results in the fact that the built SL model may not contain more than three independent parameters.

To demonstrate the reliability of data produced on the basis of the developed model description, we performed the multi-angle measurements of reflective capacity spectra in the system of vapor–lipid film–water for *p*-polarized radiation. The obtained data demonstrated good compliance with the theoretical estimates, in particular, good agreement of data obtained for *s*- and *p*-polarizations.

Reflection coefficients and reflective capacity with account of the thin surface layer

Let us consider as in [33] the problem of reflection of the flat polarized electromagnet wave from the flat border of two media with account of an anisotropic heterogeneous SL. For the sake of simplicity let us assume that the medium A, from which the radiation falls on the interface with the medium B, is the rarified gas with dielectric permittivity $\varepsilon_1 = 1$ (Fig. 1). Besides, we will assume that the SL is thin, i.e. its specific thickness is much less than the wavelength of the incident radiation λ. In [33] the expressions were obtained for the reflection coefficients R_p and R_s of reflective capacities r_p and r_s in such systems for radiation polarized in the plane of incidence (*p*-polarization), and perpendicularly to the plane of incidence (*s*-polarization). These expressions have the following form:

$$\tilde{R}_s = \tilde{R}_s^F \left\{ 1 - \frac{2\imath k_0 \cos\phi_0}{\tilde{\varepsilon}_B - 1}\, \tilde{I}_1 \right\}, \tag{1}$$

$$\tilde{R}_p = \tilde{R}_p^F \left\{ 1 - \frac{2\imath k_0 \cos\phi_0}{(\tilde{\varepsilon}_B - 1)\left(1 - \frac{1+\tilde{\varepsilon}_B}{\tilde{\varepsilon}_B}\sin^2\phi_0\right)} \times \left[\tilde{I}_1 - \left(\frac{\tilde{I}_1}{\tilde{\varepsilon}_B} + \tilde{I}_2 \right) \sin^2\phi_0 \right] \right\}, \tag{2}$$

$$r_s = r_s^F \left\{ 1 + 4k_0 \cos\phi_0\, \frac{I_{\text{eff}}^{(s)}}{(\varepsilon_B' - 1)^2 + \epsilon_B''^2} \right\}, \tag{3}$$

$$r_p = r_p^F \left\{ 1 + 4k_0 \cos\phi_0 \times \frac{I_{\text{eff}}^{(p)}}{[(\varepsilon_B' - 1)^2 + \varepsilon_B''^2][(1 - O_r \sin^2\phi_0)^2 + O_i^2 \sin^4\phi_0]} \right\}, \tag{4}$$

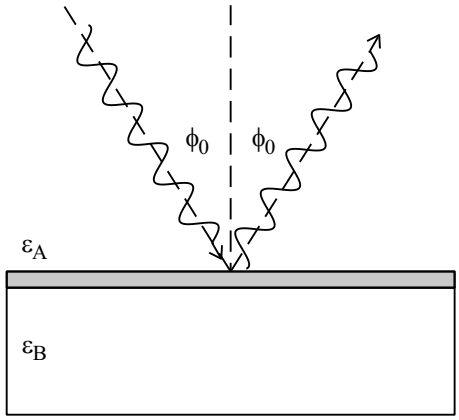

Figure 1. The optical scheme of reflection of radiation at the interface of two media A and B with the thin surface layer between them. The refracted beam is not considered in this study, therefore, its image is excluded.

Here,

$$\tilde{R}_s^F = \sin(\phi_0 - \phi_B)/\sin(\phi_0 + \phi_B)$$

and

$$\tilde{R}_p^F = \tan(\phi_0 - \phi_B)/\tan(\phi_0 + \phi_B)$$

— Fresnel reflection coefficients for a sharp step-like interface between the media for *s*- and *p*-polarized radiation, accordingly, $r_s = \tilde{R}_s \tilde{R}_s^*$ and $r_p = \tilde{R}_p \tilde{R}_p^*$, $k_0 = 2\pi/\lambda$, ϕ_0 — angle of incidence, ϕ_B — angle of refraction, $\tilde{\epsilon}_B$ — dielectric permittivity of the medium B. Hereinafter the tilde specifies the complex nature of the value.

The equations (2) and (4) are not applicable in the direct vicinity of the Brewster angle, when $\cos(\phi_0 + \phi_B)$ becomes comparable or less than the corrections from SL.

Integrals $\tilde{I}_1$ and $\tilde{I}_2$ in (1)–(4) are the only values determining the contribution of the surface optical characteristics to the reflection coefficients and reflective capacities:

$$\tilde{I}_1 = I_{1r} + \imath I_{1i} = \int_0^\infty dz \left(\tilde{\varepsilon}_t(z) - \tilde{\varepsilon}_B \right), \tag{5}$$

$$\tilde{I}_2 = I_{2r} + \imath I_{2i} = \int_0^\infty dz\, \frac{\tilde{\varepsilon}_n(z) - \tilde{\varepsilon}_B}{\tilde{\varepsilon}_n(z)}. \tag{6}$$

The tensor of dielectric permittivity in the flat surface layer $\hat{\varepsilon}(z) = \tilde{\varepsilon}_{ij}(z)\delta_{ij}$ is diagonal as a result of cylindrical symmetry, δ_{ij} — Kronecker's delta, $i, j = x, y, z$, Cartesian ordinates x and y lie in the plane of SL, Cartesian ordinate z is perpendicular to its plane. For the sake of brevity let us introduce designations $\tilde{\varepsilon}_{xx}(z) = \tilde{\varepsilon}_{yy}(z) = \tilde{\varepsilon}_t(z)$ and $\tilde{\varepsilon}_{zz}(z) = \tilde{\varepsilon}_n(z)$. Hereinafter we will designate the complex dielectric permittivities as $\tilde{\varepsilon}_i = \varepsilon_i' + \imath\epsilon_i''$, where $i = xx, yy, zz, t, n$, B.

We will name the value $\tilde{I}_1$ an integral surface excess of dielectric permittivity, and $\tilde{I}_2$ — the integral surface excess of the return dielectric permittivity. Both values are

determined by the difference of the dielectric permittivities of the surface layer and the volume medium and have the length size

$$I_{\text{eff}}^{(s)} = (\varepsilon_B' - 1)I_{1i} - \varepsilon_B'' I_{1r}, \tag{7}$$

$$I_{\text{eff}}^{(p)} = I_{\text{eff}}^{(s)} + I_{s2}\sin^2\phi_0 + I_{s4}\sin^4\phi_0, \tag{8}$$

$$I_{s2} = -\left((\varepsilon_B' - 1)I_{1i} - \varepsilon_B'' I_{1r}\right) - \left((\epsilon_B' - 1)I_{2i} - \varepsilon_B'' I_{2r}\right) - 2\frac{(\varepsilon_B' - 1)I_{1i} - \varepsilon_B'' I_{1r}}{\varepsilon_B'^2 + \varepsilon_B''^2}\varepsilon_B', \tag{9}$$

$$I_{s4} = \varepsilon_B'\frac{\varepsilon_B'^2 + \varepsilon_B''^2 - 1}{\varepsilon_B'^2 + \varepsilon_B''^2} I_{2i} - \varepsilon_B''\frac{\varepsilon_B'^2 + \varepsilon_B''^2 + 1}{\varepsilon_B'^2 + \varepsilon_B''^2} I_{2r} + \frac{\varepsilon_B'^2 - \varepsilon_B''^2 - 1}{\varepsilon_B'^2 + \varepsilon_B''^2} I_{1i} - 2\frac{\varepsilon_B'\varepsilon_B''}{\varepsilon_B'^2 + \varepsilon_B''^2} I_{1r}. \tag{10}$$

In case of normal incidence (1) matches (2), and (3) matches (4).

The surface contribution to the reflective capacity of *s*-polarized radiation is determined by value $I_{\text{eff}}^{(s)}$, the angular dependence of corrections to the Fresnel contribution is determined by the multiplier $\cos\phi_0$. The surface contribution for *p*-polarization is determined by $I_{\text{eff}}^{(p)}$. Its angular dependence in this case is quite complicated. Dependence on the angle of incidence in the denominator is determined by the volume dielectric permittivity and the angle of incidence, and its discussion is not of independent interest when discussing the surface contribution to the reflective capacity. The angular dependence of the numerator, the value of which is the one determined by the surface excesses, is determined by the three contributions proportional to $\cos\phi_0$, $\sin^2\phi_0\cos\phi_0$ and $\sin^4\phi_0\cos\phi_0$.

The value $I_{\text{eff}}^{(s)}$ is determined by excesses of the material and the imaginary parts of only the tangential component of the tensor of dielectric permittivity (5) and does not depend on the angle of incidence. The value $I_{\text{eff}}^{(p)}$ depends on the angle of incidence and is determined by the material and imaginary parts of integral excesses (5) and (6).

Determining the optical density of reflection as $a_s = -\log_{10}\frac{r_s}{r_s^F}$ and $a_p = -\log_{10}\frac{r_p}{r_p^F}$, we get

$$a_s = -\frac{4k_0\cos\phi_0}{\ln 10}\frac{I_{\text{eff}}^{(s)}}{(\varepsilon_B' - 1)^2 + \varepsilon_B''^2} \tag{11}$$

$$a_p = -\frac{4k_0\cos\phi_0}{\ln(10)} \times \frac{I_{\text{eff}}^{(p)}}{[(\varepsilon_B' - 1)^2 + \varepsilon_B''^2][(1 - O_r\sin^2\phi_0)^2 + O_i^2\sin^4\phi_0]}. \tag{12}$$

Comparing (3), (4) and (11), (12), it is possible to ascertain that the above conclusions on the contribution of surface excesses to the reflective capacities of the polarized light and their dependences on the angle of incidence are true for optical densities a_s and a_p as well. It should be emphasized that in the main approximation by the thickness of SL the values of optical densities are determined only by four integral parameters, depending on the surface characteristics, namely, the material and imaginary parts of the surface excesses (5) and (6).

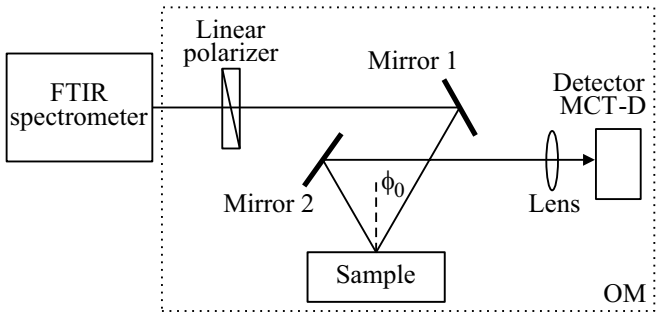

Figure 2. The optical scheme of experimental installation for measurement of the reflection absorption spectra in the IR range at different angles of incidence and polarization of light.

Experiment

Measurement of the reflection-absorption spectra at different angles of incidence and polarization of radiation was carried out using IR Fourier spectrometer Nicolet 8700 (Thermo Fisher Scientific), equipped with an external optical module (OM) with the receiver MCT-D. The experimental scheme of installation is shown in Fig. 2. Infrared radiation from the spectrometer is directed to the external optical module OM. The linear polarizer and mirrors *1* and *2* are fixed on the motorized translators, which makes it possible to automatically specify the necessary *s*- or *p*-polarization and the angle of incidence ϕ_0 of light. The light reflected from the interface of water–thin film–water vapor is directed using the mirror *2* and the optical lens to the cathode of the receiver MCT-D. The reflection absorption spectra were measured in the range of $1000–4000\,\text{cm}^{-1}$ with resolution $2\,\text{cm}^{-1}$ and averaging by 1024 measurements.

Multi-angle measurements of the reflective capacity were performed for the interval of the angles of incidence 20–50° from three samples of water with the applied film of dipalmitoylphosphatidylcholine (DPPC), the surface density is $0.49\,\text{nm}^2/\text{mol}$. Measurements started in 1.5 hours after installation of the sample in the OM and application of the film. The temperature in the OM was $23 \pm 0.5^{\circ}\text{C}$.

Results and discussion

The measured reflection-absorption spectra made it possible to calculate the spectra of optical density in the interval of wave numbers $1000–4000\,\text{cm}^{-1}$. In Fig. 3 the dependence of the optical density on the wave number

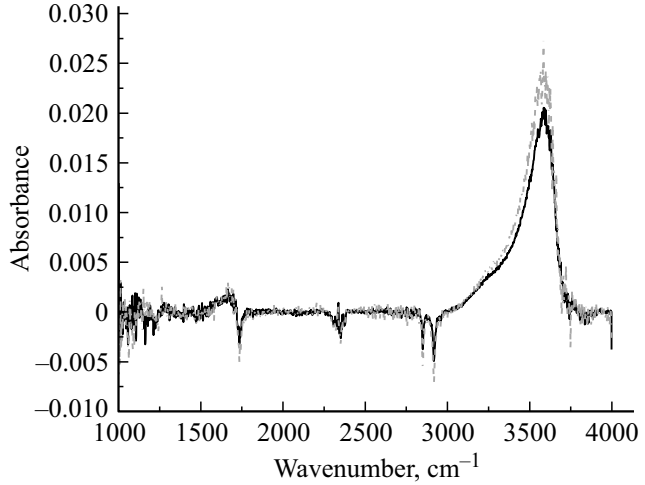

Figure 3. The spectra of optical density calculated from experimental data for DPPC at angle of incidence 30°, *s*-polarization (solid curve), *p*-polarization (dotted line).

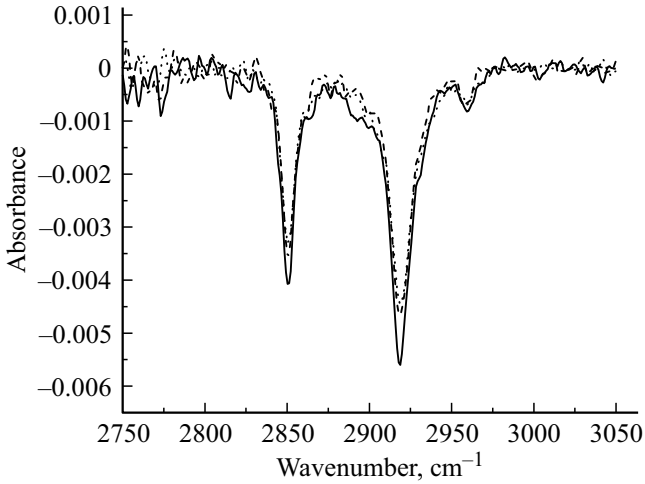

Figure 4. The spectra of optical density calculated on the basis of experimental data for DPPC at angles of incidence 20 (solid curve), 30 (dashed curve), 40° (dotted line) for *s*-polarization.

is presented for both polarizations at the angle of incidence 30°.

This paper studies in detail the symmetric (2850 cm^{-1}) and antisymmetric (2919 cm^{-1}) methylene bands, which are convenient both from the point of view of a quite high absorption ratio and significant distance from other resonances. Discussion of other bands, first of all, related to the water spectra in the volume and vapor phases, is of obvious interest, but is not included in the objectives of this paper.

The calculated spectra of optical density of both polarizations for the angles of incidence 20, 30 and 40° are presented in Fig. 4, 5 and 6. From the figures it can be seen that the bands in case of *p*−polarization are much larger in amplitude than *s*-polarizations. Besides, in accordance with the above consideration, the intensity of these bands increases noticeably when approaching the Brewster angle. In case of *s*-polarization the dependence of the optical density on the angle is relatively low, since according to (11) it is defined by the cosine of the angle of incidence. For comparison, in Fig. 6 there are spectra of optical density for *s*- and *p*-polarized radiation at angle of incidence 40°.

Note that the amplitude of maxima for the specified bands differs more than twice. Since at narrow angles of incidence under the general assumptions the maxima are close in value, it is obvious that this difference is caused by faster growth of the optical density for *p*−polarized light upon increase of the angle of incidence compared to the case of *s*−polarized radiation.

The experimental data make it possible to determine the values $I_{\text{eff}}^{(s)}$ and $I_{\text{eff}}^{(p)}$. The results are shown in Fig. 7, 8.

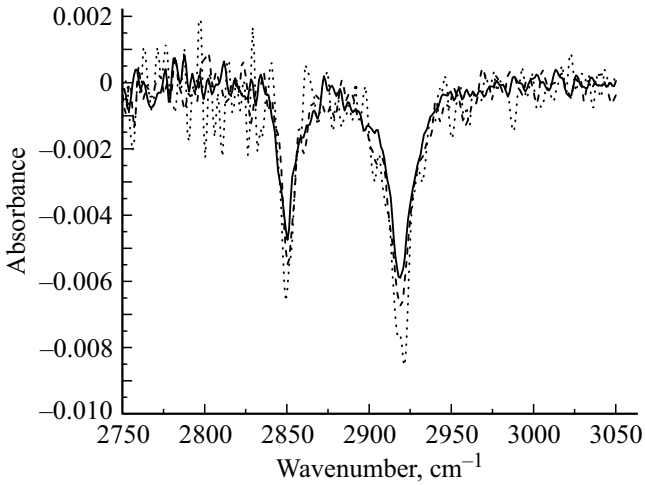

Figure 5. The spectra of optical density calculated on the basis of experimental data for DPPC at angles of incidence 20 (solid curve), 30 (dashed curve), 40° (dotted line) for *p*-polarization.

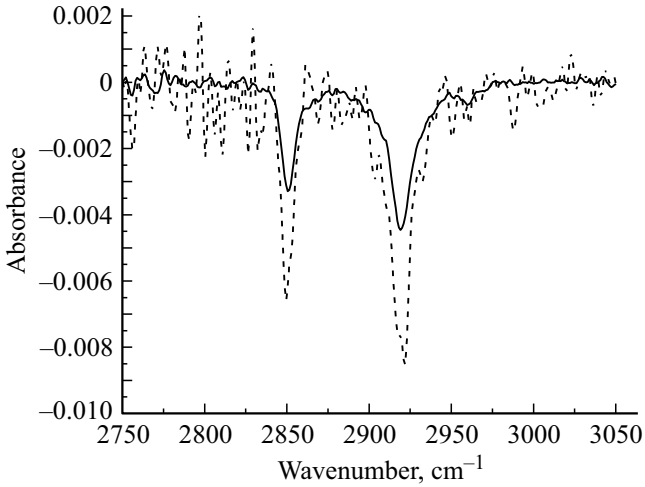

Figure 6. The spectra of optical density calculated on the basis of experimental data for DPPC at angles of incidence 40° for *s*- (solid curve) and *p*- (dashed curve) of polarized radiation.

In accordance with (7) $I_{\text{eff}}^{(s)}$ dos not depend on the angle of incidence, which corresponds to the experimental data of Fig. 7, which provide the results for the maxima of symmetric and antisymmetric methylene bands produced for various angles of incidence. The values of dielectric permittivity of water necessary for calculations were taken from the paper [41]. The results of data processing yield the average values of maxima $2850.5 \pm .0.4$ and $2918.8 \pm 0.4\,\text{cm}^{-1}$ positions, and the average $I_{\text{eff}}^{(s)}$ 1.08 ± 0.04 and $1.60 \pm 0.03\,\text{nm}$ for the symmetric and antisymmetric bands, accordingly.

The value $I_{\text{eff}}^{(p)}$ depends on the angle of incidence and contains summands proportional to $\sin^{2j}\phi_0$, $j = 0, 1, 2$.

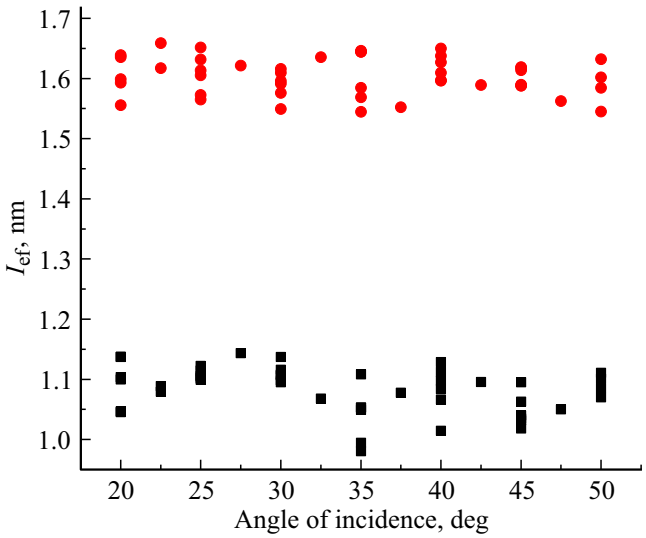

Figure 7. The value $I_{\text{eff}}^{(s)}$ calculated from the experimental data for antisymmetric (circles) and symmetric (squares) methylene bands at different angles of incidence for $s-$polarization.

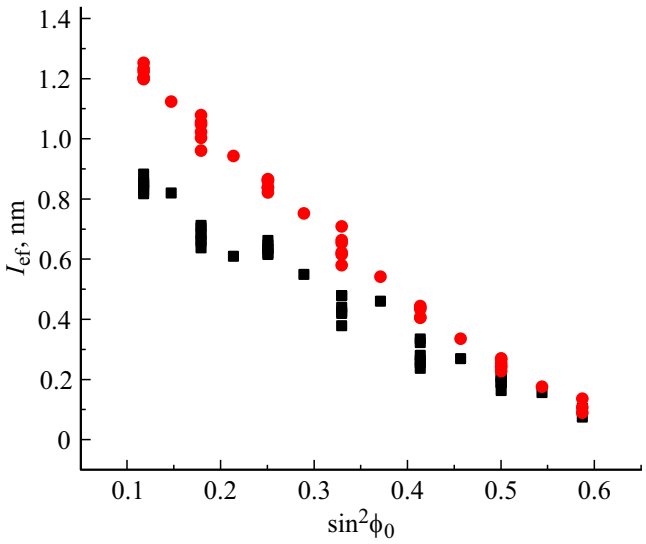

Figure 8. The value $I_{\text{eff}}^{(p)}$ calculated from the experimental data for antisymmetric (circles) and symmetric (squares) methylene bands at different angles of incidence for $p-$polarization.

The values (nm) of three integral parameters produced for symmetric ω_1 and antisymmetric ω_2 methylene bands

Polarization	$I_{\text{eff}}^{(s)}$	I_{s2}	I_{s4}
ω_1	1.07 ± 0.04	-2.2 ± 0.2	0.8 ± 0.3
ω_2	1.61 ± 0.05	-3.5 ± 0.3	1.5 ± 0.4

It should be noted that the contribution to $I_{\text{eff}}^{(p)}$ at $j = 0$ is determined by $I_{\text{eff}}^{(s)}$. The average values of the band maxima positions obtained from experimental data processing for $p-$polarized radiation: 2850.2 ± 0.7 and $2919.3 \pm 1.1\,\text{cm}^{-1}$; the results for $I_{\text{eff}}^{(p)}$ are provided in the table.

The values for the position of bands produced by both polarizations are well agreed with each other and the references [3,17,18].

Comparing values $I_{\text{eff}}^{(s)}$, calculated from the measurement results for $s-$ and $p-$polarizations, one may note that they match well. It means in particular that the measurements for $s-$polarized radiation provide no additional data in respect to the results obtained by using $p-$polarization. The error value in the case of $p-$polarization is higher since it is explained by the low reflective capacity in this case.

The accuracy of determination of I_{s2} and I_{s4} is noticeably lower than for the value of $I_{\text{eff}}^{(s)}$, which is due to the relatively narrow interval of angles of incidence. In accordance with (8) the analysis of angular dependence of $p-$polarized light makes it possible to calculate only three values: $I_{\text{eff}}^{(s)}$, I_{s2} and I_{s4}. Therefore, using measurements of optical density will not allow for calculation of the material and imaginary parts of the surface excesses (5) and (6). The developed models of the surface layer structure must be agreed with the experimentally measured values $I_{\text{eff}}^{(s)}$, I_{s2} and I_{s4}.

Conclusion

Based on the obtained experimental data, it is possible to conclude that the reflection-absorption spectroscopy in the main approximation by the thickness of film makes it possible to determine the three parameters set by excesses of dielectric permittivity in SL. As a result, when discussing it structure, the model shall not contain more than three parameters. The proposed film models must comply with their experimentally found values.

The study of the optical density during reflection of $s-$polarized radiation provides no additional information in addition to the one obtained from analysis of optical density of $p-$polarized light. Multi-angle measurements at $s-$polarization may only help to improve the measurement accuracy. Nevertheless, measurement of reflection of $s-$of polarized radiation may be used to align the device. In this case the criterion of proper optical tuning will be the

stability of the angular invariant determined for various angles of light incidence.

Funding

This study was financially supported by the Russian Science Foundation, grant №23-22-00035, https://rscf.ru/project/23-22-00035/.

Conflict of interest

The authors declare that they have no conflict of interest.

References

[1] E.C. Griffith, T.R.C. Guizado, A.S. Pimentel, G.S. Tyndall, V. Vaida. The Journal of Physical Chemistry, C **117**, 22341 (2013).
[2] C.P. Baryiames, P. Garrett, C.R. Baiz. The Journal of Chemical Physics, **154**, 170901 (2021).
[3] F. Strati, R. Reinhard, H.H. Neubert, L. Opalka, A. Kerth, G. Brezesinski. European Journal of Pharmaceutical Sciences, **157**, 105620 (2021).
[4] N. Nagai, H. Okada, T. Hasegawa. AIP Advances, **9**, 105203 (2019).
[5] N. Chirkov, R. Campbell, A. Michailov, P. Vlasov, B. Noskov. Polymers, **13**, 2820 (2021).
[6] S. Gromelski, G. Brezesinski. Langmuir, **22**, 6293 (2006).
[7] C. Stefaniu, G. Brezesinski, H. Möhwald. Advances in Colloid and Interface Science, **208**, 197 (2014).
[8] V. Lyadinskaya, S.-Y. Lin, A. Michailov, A. Povolotskiy, B. Noskov. Langmuir, **32**, 13435 (2016).
[9] R. Mendelsohn, G. Mao, C.R. Flach. Biochimica et Biophysica Acta, **1798**, 788 (2010).
[10] M. Hoffmann, S. Drescher, C. Schwieger, D. Hinderberger. Phys. Chem. Chem. Phys., **23**, 5325 (2021).
[11] A. Malik, P. Seeberger, G. Brezesinski, D. Silva. Chem. Phys. Chem., **22**, 757 (2021).
[12] M. Krycki, S.-Y. Lin, G. Loglio, A. Michailov, R. Miller, B. Noskov. Colloids and Surfaces B: Biointerfaces, **202**, 111657 (2021).
[13] W. Zhao, M. Goethelid, S. Hosseinpour, M. Johansson, G. Li, C. Leygraf, C. Johnson. Journal of Colloid and Interface Science, **581**, 816 (2021).
[14] F. Petersen, I. Lautenschlaeger, A. Schlimm, B. Floeser, H. Jacob, R. Amirbeigiarab, T.R. Rusch, T. Strunskus, O. Magnussen, F. Tuczek. Dalton Transactions, **50**, 1042 (2021).
[15] L. Noc, M. Licen, I. Drevensek-Olenik, R. Chouhan, J. Kovac, D. Mandler, I. Jerman. Solar Energy Materials and Solar Cells, **223**, 110984 (2021).
[16] A. Gericke, A. Michailov, H. Huhnerfuss. Vibrational Spectroscopy, **4**, 335 (1993).
[17] C. Flach, Z. Xu, X. Bi, J. Brauner, R. Mendelsohn. Applied Spectroscopy, **55** (8), 1060 (2001).
[18] C. Schwieger, B. Chen, C. Tschierske, J. Kressler, A. Blume. J. Phys. Chem. B, **116**, 12245 (2012).
[19] X. Wang, X. Huang, Y. Xin, X. Du. Phys. Chem. Chem. Phys., **14**, 5470 (2012).
[20] C. Roldan-Carmona, C. Rubia-Paya, M. Perez-Morales, M. Martın-Romero, J. Giner-Casares, L. Camacho. Phys. Chem. Chem. Phys., **16**, 4012 (2014).
[21] E. Koepf, R. Schroeder, G. Brezesinski, W. Friess. Journal of Pharmaceutics and Biopharmaceutics, **119**, 396 (2017).
[22] T. de los Arcos, H. M.uller, F. Wang, V.R. Damerla, C. Hoppe, C. Weinberger, M. Tiemann, G. Grundmeier. Vibrational Spectroscopy, **114**, 103256 (2021).
[23] N.M. Azzam, R.M.A. Bashara. *Ellipsometry and Polarized Light* (North-Holland Personal Library, 1999).
[24] F. Picard, T. Buffeteau, B. Desbat, M. Auger, M. Pezolet. Biophysical Journal, **76**, 539 (1999).
[25] J. McIntyre, D. Aspens. Surface Science, **24**, 417 (1971).
[26] J. McIntyre. Surface Science, **37**, 658–682 (1973).
[27] D. Kolb, J. McIntire. Surface Science, **28**, 321 (1971).
[28] T. Buffeteau, B. Desbat, J.M. Turlet. Applied Spectroscopy, **45**, 380 (1991).
[29] V.P. Tolstoy. *Vvedenie v opticheskuyu adsorbtsionnuyu spectroskopiyu nanorazmernykh materialov* (Solo, 2014) (in Russian).
[30] V.L. Kuzmin, A.V. Michailov. Opt. Spectrosc. (USSR), **51**, 383 (1981).
[31] V.L. Kuzmin, V.P. Romanov, A.V. Michailov. Opt. Spectrosc (USSR), **73**, 1 (1992).
[32] V. Kuzmin, V. Romanov, L. Zubkov. Phys. Rep. **248**, 71 (1994).
[33] A. Mikhailov, V.L. Kuzmin. Optics and Spectroscopy **128**, 404 (2020).
[34] C. Flach, A. Gericke, R. Mendelsohn. J. Phys. Chem. B, **101**, *58*, 101 (1997).
[35] Z. Xu, J. Brauner, C. Flach, R. Mendelsohn. Langmuir, **20**, 3730 (2004).
[36] H. Wang, W. Miao, H. Liu, X. Zhang, X. Du. J. Phys. Chem. B, **114**, 11069 (2010).
[37] C. Schwieger, X. Liub, M. Krafft. Phys. Chem. Chem. Phys., **19**, 23809 (2017).
[38] M. Hoernkea, J. Mohand, E. Larssone, J. Blomberge, D. Kahrae, S. Westenhoffa, C. Schwiegerf, R. Lundmark. PNAS Direct Submission, **22**, 4360 (2017).
[39] A. Michaylov, A. Povolotskiy, V. Kuzmin. Optics Express, **29**, 3090 (2021).
[40] N.N. Rozanov, V.M. Zolotarev. Opt. i spektr., **49**, 925 (1980).
[41] J.E. Bertie, M.K. Ahmed, H.H. Eysel. J. Phys. Chem., **93**, 2210 (1989).

Translated by M.Verenikina